Journal of Applied Fluid Mechanics, Vol. 10, No. 3, pp. 881-887, 2017.
Available online at www.jafmonline.net, ISSN 1735-3572, EISSN 1735-3645.
DOI: 10.18869/acadpub.jafm.73.240.27056

Vorticity-Based Study of Apparent Mass of Body of Revolution

X. Fu[1†], A. Y. Mao[2] and Z. Z. Jin[2]

[1] *J. C. Wu Center for Aerodynamics, School of Aeronautics and Astronautics, Shanghai Jiao Tong University, Shanghai, China*
[2] *Shanghai Haiying Machinery Factory, Shanghai, China*

†*Corresponding Author Email: fuxiang1987@sjtu.edu.cn*

(Received August 12, 2016; accepted January 24, 2017)

ABSTRACT

The apparent mass effect is enhanced significantly when the motion of a body changes quickly, such as a flapping wing or an impulsively started plate. Previous method for calculating the apparent mass of a given body needs to adopt the assumption of ideal flow and know the potential of velocity field arising in the fluid due to the motion of the body. However, the assumption of ideal flow is contrary to real fluid field and it is hard to obtain the potential of velocity field in most cases. In this paper, a new method based on the vorticity moment theorem for calculating the apparent mass of the body of revolution in the axial direction due to axial acceleration is developed. This method has no assumption of ideal flow and establishes the relationship between the apparent mass and the vorticity loops adjacent to the surface of the body. Using this method, the value of the apparent mass can be easily figured out and the physical mechanism of the apparent mass can be revealed from the view of the vorticity loop. The comparisons between different bodies have shown the influences of the fineness ratio (the ratio of the length to the maximum diameter) and the trailing edge type on the apparent mass.

Keywords: Apparent mass; Vorticity loop; Vorticity moment.

NOMENCLATURE

A_i	area enclosed by the vorticity loop i
$\mathbf{a}$	acceleration vector
a	acceleration in the axial direction
c_i	contribution of the vorticity loop i
d_t	time interval
d_v	terminal velocity
$\mathbf{F}$	instantaneous aerodynamic force
$\mathbf{F}a$	apparent mass force
Fa_z	apparent mass force in the axial direction
k_z	apparent mass coefficient
L_i	integral path enclosing the core of the vorticity loop i
$\mathbf{n}_i$	normal vector of the cross-section of the vorticity loop i
m_z	apparent mass in the axial direction
m_f	mass of the fluid displace by the solid body
r	position vector
R_S	region occupied by the solid body
R_∞	infinite unlimited space occupied jointly by the fluid and solid
S	surface of the solid body
S^*	surface around the solid body
S_i	perimeter of the vorticity loop i
t	physical time
v	velocity vector
V_r	r component of the velocity induced by the ordinary sub-belt
V_z	z component of the velocity induced by the ordinary sub-belt
V_r'	r component of the velocity induced by the singular sub-belt
V_z'	z component of the velocity induced by the singular sub-belt
V_r''	r component of Cauchy principal value
V_z''	z component of Cauchy principal value
ω	vorticity of the fluid
Γ_i	circulation of the vorticity loop i

1. INTRODUCTION

When a body accelerates in a fluid, it will be imposed by an additional inertial force, which could be attributed to an equivalent apparent mass of fluid. In 1776, the notion of apparent mass was first introduced by Dubua (Birkhoff 1960), who experimentally investigated the oscillating

pendulum. In 1843, Stokes studied the motion of a sphere in an ideal infinite fluid and an exact analytical expression for the apparent mass of a sphere was obtained (Lamb 1932). In his article, the apparent mass was simply interpreted by the effect of the fluid pressure. Later, the apparent mass of an arbitrary body moving in different regimes was figured out by the effort of many researchers. In 1986, Lighthill noted the apparent mass may represent a negligible addition to the normal mass of a solid body which immersed in a fluid and the apparent mass properties only depend on the shape and the direction of acceleration of the solid body (Lighthill 1986). However, in some cases, the apparent mass may play a very important role during the motion of the body. It is shown that the apparent mass has a great effect on the motion of an airship because it may be close to the actual mass of the airship itself (Li and Nahon 2007). Another interesting case is the unsteady motion of the wing in nature. With the apparent mass force associated with a high acceleration rate, a large lift peak can be obviously obtainable by very rapid accelerations of a model fruit fly wing (Sane and Dickinson 2002).

The most popular traditional way to find out the apparent mass of a solid body is the potential flow method. The method first assumes a body moves in an infinite ideal fluid, and then gets the total kinetic energy of the fluid when the whole velocity field is known, finally the apparent mass can be calculated out through the relation between the force and the kinetic energy (Lamb 1932). For some special bodies, such as ellipsoids, thin plates and Rankine bodies, the apparent masses can be obtained easily because the velocity fields around these bodies have analytic solutions. However, apart from these special bodies, the apparent masses of unconventional bodies are usually calculated by approximation for the difficulty of solving the velocity fields. Due to the limitation and complication of computation and the unrealistic assumption of the ideal flow, the potential flow method is not able to reveal the physical mechanism of the apparent mass. In fact, all the traditional methods need the assumption of the ideal flow.

The vorticity moment theorem was developed by Wu (1981), which is able to relate the aerodynamic load to the moment of the vorticity of the whole system. Under the guidance of the theorem, Wang and Wu (2010) and Li and Lu (2012) studied the relationship between the aerodynamic force and the vortex ring shed from a flapping wing, Tian *et al*. (2016) investigated the effect of the wake vortices on the propulsion performance of a pitching airfoil, Li and Wu (2016) discussed the vortex force generation for a flat plate at arbitrarily large angle of attack. As mentioned in the vorticity-moment theorem (Wu 1986), there is a layer of vorticity appears immediately adjacent to the surface of the solid body when it accelerates suddenly in the fluid from rest, and then the apparent mass and the apparent mass force could be easily obtained through the total first moment of all the vorticity in the layer. This definition does not involve the assumption of the ideal flow and points out the origin of the apparent mass force. However, few works had been done with the study of the apparent mass using the theorem.

In this article, a new method based on the vorticity moment theorem will be derived for calculating the apparent mass of the revolution body. The new method simplifies the layer of vorticity adjacent to the surface of the solid body into a set of coaxial vorticity loops and then establishes the relationship between the apparent mass and the vorticity loops. In the following, the definitions of the apparent mass from the view of vorticity moment theorem will be stated in section 2. The derivation process of the new method will be presented in section 3. Section 4 shows the procedure for calculating the circulation distribution of the vorticity loops. The validation of the new method and some discussion will be given in section 5. The main conclusions are enumerated in section 6.

2. APPARENT MASS EXPRESSED BY VORTICITY MOMENT THEOREM

The vorticity moment theorem was developed by Wu in 1981 (Wu 1981). It is a general aerodynamic theory for the calculation of force and moment. According to this theory, the instantaneous aerodynamic force F exerted on a body with a surface S moving in an incompressible stationary fluid can be expressed by

$$F = -\frac{\rho}{2}\frac{d}{dt}\iiint_{R_\infty} r\times\omega dS + \rho\frac{d}{d_t}\iiint_{R_S} vdR. \qquad (1)$$

where ρ is the density of fluid, v is the velocity vector, ω is the vorticity, r is the position vector, Rs is the region occupied by the solid body, R_∞ is the infinite unlimited space occupied jointly by the fluid and the solid.

Equation (1) relates the instantaneous aerodynamic force to the rate of the change of the total first moment of vorticity in R_∞. As implied by Wu (1981), every vorticity field in the infinite unlimited space occupied jointly by solid and fluid is portrayable by a set of vorticity loops. So the aerodynamic force can be divided into different parts contributed from some special vorticity loops.

If a solid body accelerating suddenly from rest in an infinite large and quiescent fluid during the time interval dt, there is a vorticity layer appears in the fluid immediately adjacent to the surface S of the solid body which satisfies the no-slip boundary condition on S. The time interval dt is too small to transport of the vorticity in the layer by diffusion and convection, so the layer is very thin and can be approximated by a sheet of vorticity on S_*, a surface surrounding the solid body. The vorticity is zero outside the sheet and the vorticity distribution ω of the sheet can be uniquely determined by the known velocity on S.

According to the vorticity moment theorem, the apparent mass force F_a is linked to the rate of the change of the total first moment of vorticity in the sheet adjacent to the body surface and can be figured out using this equation (Wu 1986):

$$F_a = -\frac{\rho}{2}\frac{d}{dt}\iiint_{S^*} r \times \omega dS + \rho\frac{d}{d_t}\iiint_{R_s} v dR. \quad (2)$$

The force F_a is a resistance to acceleration, so it is conveniently interpreted as an effect of apparent mass. Compared with the potential flow method, the definition by the vorticity moment theorem has no simplifying assumptions, especially the assumption of ideal flow. Moreover, the physical mechanism of the apparent mass can be well explained by the vorticity moment theorem.

3. APPARENT MASS OF THE BODY OF REVOLUTION

Apparent mass properties are tensorial which have 36 values and only 21 values are independent (Korotkin 2007). In this section, a new method calculating for the apparent mass of the body of revolution in the axial direction due to axial acceleration will be derived using the vorticity moment theorem.

Consider a body of revolution accelerating to a velocity of dv = 1 in the axial direction from rest. The acceleration of the body a is infinitely large and the time interval dt is infinitesimally small. The layer of vorticity adjacent to the surface of the body generated during the process is first divided into N vorticity belts. Then each belt is approximated to an axisymmetric vorticity loop located at the middle of the corresponding belt. The radius of the core of each loop is infinitesimally small. The vorticity belts and the vorticity loops are displayed in Fig. 1 and the cylindrical coordinate system is taken.

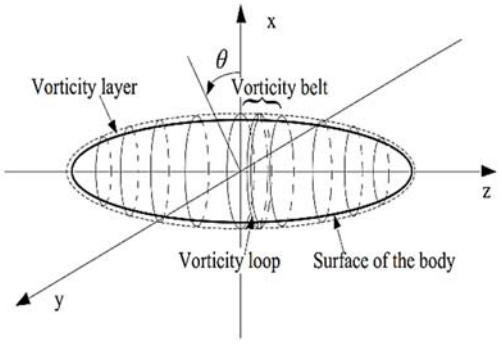

Fig. 1. Illustration of vorticity belts and vorticity loops.

Assume now the circulation of the vorticity loop i is Γ_i. Using Stokes' theorem, the relationship between circulation and vorticity field of the loop i is:

$$\iint_{W_i} \omega.n_i dA = \oint_{Li} v.ds = \Gamma_i, \quad (3)$$

where W_i is the cross-section of the vorticity loop i, ni is the normal vector of section Wi and the integral path L_i is an arbitrarily chosen loop enclosing the core of the vorticity loop i, as described in Fig. 2.

Equation (2) can be rewritten here as:

$$F_a = -\frac{\rho}{2}\sum_{i=1}^{N}\frac{d}{dt}(\oint_{W_i} \omega dA)dI + \rho\frac{d}{dt}\iiint_{R_s} v dR, \quad (4)$$

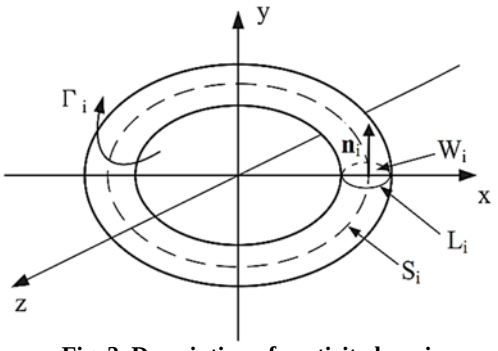

Fig. 2. Description of vorticity loop i.

where the integral path Si is the perimeter of the loop i.

Using Eq. (3) and note that the last term in Eq.(4) is actually the product of the mass of the fluid displaced by the body and the acceleration of the body, equation (4) becomes:

$$F_a = -\frac{\rho}{2}\sum_{i=1}^{N}\frac{d}{dt}(\Gamma_i \oint_{L_i} r \times dI) + m_f a, \quad (5)$$

where mf is the actual mass of the fluid occupied by the body, a is the acceleration vector of the solid body.

Thus the apparent mass force in the axial direction can be easily obtained by projecting Fa onto the axial direction:

$$Fa_z = -\rho\sum_{i=1}^{N}\frac{d}{dt}(\Gamma_i A_i) + m_f a, \quad (6)$$

where A_i is the area enclosed by the vorticity loop i, a is the acceleration in the axial direction.

According to the definition of apparent mass in the axial direction:

$$Fa_z = -m_z a, \quad (7)$$

the apparent mass in the axial direction is given by:

$$m_z = \frac{-\rho\sum_{i=1}^{N}\frac{d}{dt}(\Gamma_i A_i) + m_f a}{-a} \quad (8)$$

Note that dv=1, and

$$dv = adt, \quad (9)$$

$$m_z = \rho\sum_{i=1}^{N}\left[(\Gamma_i A_i)_{t=dt} - (\Gamma_i A_i)_{t=0}\right] - m_f. \quad (10)$$

Because there is no vorticity exists on the body surface before the acceleration, equation (10) becomes:

$$m_z = \rho \sum_{i=1}^{N} (\Gamma_i A_i)_{t=dt} - m_f . \tag{11}$$

For brevity, the subscript "t = dt" is dropped and Eq. (11) becomes:

$$m_z = \rho \sum_{i=1}^{N} (\Gamma_i A_i) - m_f . \tag{12}$$

Equation (12) shows that the apparent mass of the body of revolution in the axial direction could be represented by the product of the circulation and area of each vorticity loop. Here, a new non-dimensional coefficient c is defined to evaluate the contribution of each vorticity loop to the total apparent mass. The contribution of vorticity loop i can be expressed by:

$$c_i = \frac{\Gamma_i A_i}{\sum_{i=1}^{N} (\Gamma_i A_i)}, \tag{13}$$

The apparent mass coefficient k_z is also used here to compare the apparent mass of different bodies and can be obtained by dividing mf into mz:

$$K_z = \frac{\sum_{i=1}^{N} (\Gamma_i A_i)}{V} - 1, \tag{14}$$

where V is the volume of the revolution body.

4. CALCULATION OF THE VORTICITY LOOPS

The surface singularity method (Smith and Pierce 1958) is used to calculate the circulation of each vorticity loop in Eq. (12), (13) and (14). Different from Smith and Pierce (1958), the body of revolution is replaced by a set of coaxial vorticity loops, not the ring sources.

Consider a body approximated by N vorticity loops in the cylindrical coordinate system, the two components of the velocity V induced by loop i with circulation Γi at a control point P(r,z,θ) as shown in Fig. 3 is given by Rayner (1979):

$$V_r = \frac{\Gamma_i r_0 (z - z_0)}{4\pi} \frac{4}{[(r + r_0)^2 + (z - z_0)^2]^{\frac{3}{2}}} H(k), \tag{15}$$

$$V_r = \frac{\Gamma_i r_0}{4\pi} \frac{4}{[(r + r_0)^2 + (z - z_0)^2]^{\frac{3}{2}}} [r_0 G(k) - r H(k)], \tag{16}$$

Where

$$G(k) = E(k)(1 - K^2), \tag{17}$$

$$H(k) = \frac{1}{k^2}\left[\frac{2 - k^2}{1 - k^2} E(k) - 2K(k)\right], \tag{18}$$

K(k) and E(k) are the complete elliptic integrals of the first and second kind respectively and the argument k is given by:

$$k^2 = \frac{4 r r_0}{(r + r_0)^2 + (z - z_0)^2}. \tag{19}$$

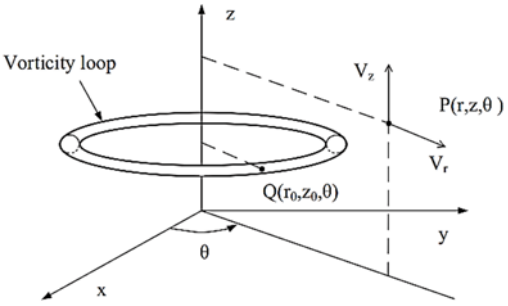

Fig. 3. Velocity induced by a vorticity loop.

If k → 0, corresponding to points near the z axis or to points in the far field, the following expressions are used for functions G(k) and H(k):

$$G(k) = \frac{1}{2}\pi\left(1 + \frac{3}{4}k^2 + \frac{4}{6}\frac{5}{4}k^4\right) \quad for \quad k^2 < 0.05 \tag{20}$$

$$H(k) = \frac{1}{2}\pi k^2\left(1 + \frac{5}{4}k^2\right) \quad for \quad k^2 < 0.01 \tag{21}$$

The self-induced velocity, which means the point P coincides with the loop i, can not be calculated directly through Eqs. (15) and (16) due to the singular problem. Inspired by Smith and Pierce (1958), the vorticity belt will not be approximated by a sole loop, but was first divided into two portions. One is the singular sub-belt within the distance d of the control point located at the middle of the belt and another is the ordinary sub-belt which located farther than d from the control point, which described in Fig. 4. Then each sub-belt will be approximated by a vorticity sub-loop. The velocity induced by the sub-loop corresponding to the ordinary sub-belt can be calculated directly through Eqs. (15) and (16). The velocity induced by the sub-loop corresponding to the singular sub-belt will be evaluated by expanding Eqs. (15) and (16) in terms of d/r_0 and integrated from s = −d to s = +d as explained in Smith and Pierce (1958). So the contributions of the sub-loop corresponding to the singular sub-belt to the induced velocity are:

$$V_r' = \frac{1}{2\pi}\frac{\Gamma_i}{\Delta s}\{\sin\beta\cos\beta S' - [\frac{1}{48}\sin\beta\cos\beta(-2\sin^2\beta + 9 + 6\ln\frac{S'}{8})]S'^3\}, \tag{22}$$

$$V_r' = \frac{1}{2\pi}\frac{\Gamma_i}{\Delta s}\langle(-\sin^2\beta + \ln\frac{S'}{8}S' + \{[\frac{1}{144}\sin^2\beta(-6\sin^2\beta - 72\cos\beta + 23 + 12\ln\frac{S'}{8}) - \frac{1}{16}(1 + \ln\frac{S'}{8})]\}S'^3\rangle, \tag{23}$$

Table 1 Apparent mass coefficients of the Rankine body and the sphere as a function of the number of loops N

	N = 80	N = 100	N = 120	N = 200	Analytical result (Milne-Thomson 1968)
Sphere	0.4871	0.4903	0.4990	0.4993	0.5
Rankine body	0.2058	0.2061	0.2077	0.2079	0.2084

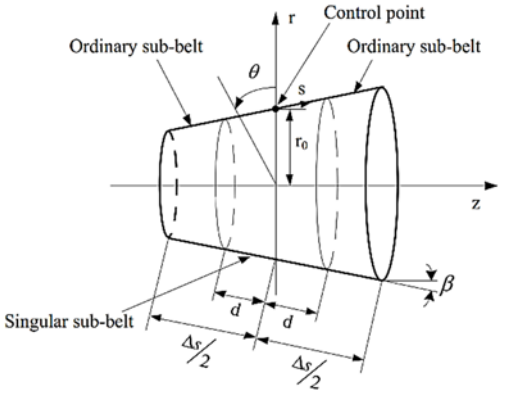

Fig. 4. Illustration of ordinary and singular sub-belts.

Where

$$S' = \frac{d}{r_0}. \tag{24}$$

The distance d is taken as d = 0.08r0 if $0.08r_0 < \Delta/2$ and d = Δs/2 if $0.08r_0 > \Delta s/2$.

Finally the contributions from Cauchy principal integral resulting from the limiting process of approaching the surface are

$$v_r'' = \frac{\Gamma_i}{2\Delta s}\sin\beta. \tag{25}$$

$$v_z'' = \frac{\Gamma_i}{2\Delta s}\cos\beta. \tag{26}$$

Thus the self-induced velocity of vorticity loop i consists of the sum of the three parts: the numerical integration of the Eqs. (15) and (16) over the ordinary sub-loops, Eqs. (22) and (23) for the effect of the singular sub-loop and the Cauchy principal integral shown in Eqs. (25) and (26).

According to the no-slip boundary condition, the tangential velocity at the control point induced by all the vorticity loops equals to the tangential velocity of the solid body. Using Eqs. (15) and (16),(22) and (23), (25) and (26), the circulation of each vorticity loop can be determined.

5. VALIDATION AND DISCUSSION

5.1 Validation of the New Method

In order to validate the new method using the vorticity moment theorem, a sphere and a Rankine body displayed in Fig. 5 are tested first. The fineness ratio of the Rankine body is set to 2. Each body is approximated by 80, 100, 120, 200 loops respectively and the new method is used to figure out the apparent mass coefficient in the axial direction due to axial acceleration. As illustrated before, the apparent mass tensors for sphere and Rankine body can be analytically derived by the potential flow method. Table 1 lists the results obtained by the new method as a function of the number of loops N (the corresponding analytical results are also shown). The agreement between numerical and analytical values is very good. The corresponding error in the calculation is less than 1% for N = 120 and N = 200. So the new method gives an excellent way to calculate the apparent mass.

5.2 Some Discussion about the Apparent Mass

The new method not only tells us the apparent mass of the body but also provides us an efficient way to study the physical mechanism of the apparent mass from the view of vorticity. In the following, the influence of the fineness ratio and the trailing edge type on the apparent mass will be discussed using the new method.

First, the sphere (fineness ratio is 1) and the Rankine body (fineness ratio is 2) displayed in Fig. 5 are

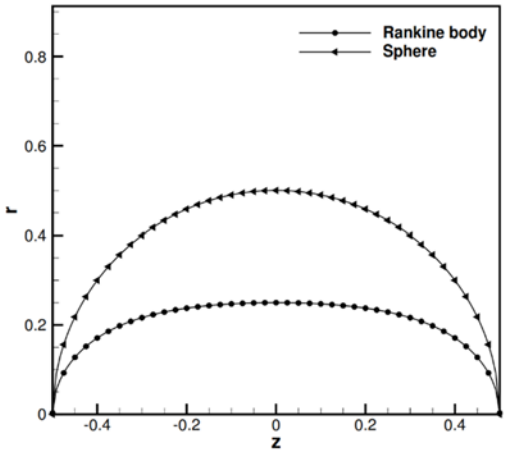

Fig. 5. Profiles of the Rankine body and the sphere.

compared for investigating the influence of the fineness ratio, where each body is approximated by 120 loops. The apparent mass coefficients of the both bodies can be found in Table 1. Fig. 6(a) shows the circulation of each loop of the sphere and the Rankine body. The circulations of the vorticity loops of the sphere are almost same except the loops

located at the two sides. To the Rankine body, the circulations of the vorticity loops located at the middle become smaller from the two sides. The circulations of the vorticity loops of the sphere are generally larger than that of the Rankine body. So a larger fineness ratio of the body causes smaller circulations of the vorticity loops. It is implied by the vorticity moment theorem that the apparent mass is determined by the product of the circulation and area of the vorticity loop. Using Eq. (12) and consider the areas of the loops of the sphere are also larger than that of the Rankine body, it is obviously that the sphere with a smaller fineness ratio has a larger apparent mass coefficient than that of the Rankine body. Fig. 6(b) shows the contribution of each loop of the two bodies to the apparent mass using Eq. (13). To the both bodies, the vorticity loops located at the middle of the body play a more important role than the loops located at the sides of the body in the generation of the apparent mass. This is because the vorticity loops located at the middle have much larger areas than the loops located at the two sides even if the circulations of the vorticity loops located at the middle of the both bodies are equal or smaller than the circulations of the loops at the two sides. So the efficient way to change the apparent mass coefficient of a body is to change the fineness ratio of the body, especially to change the maximal areas of the cross sections.

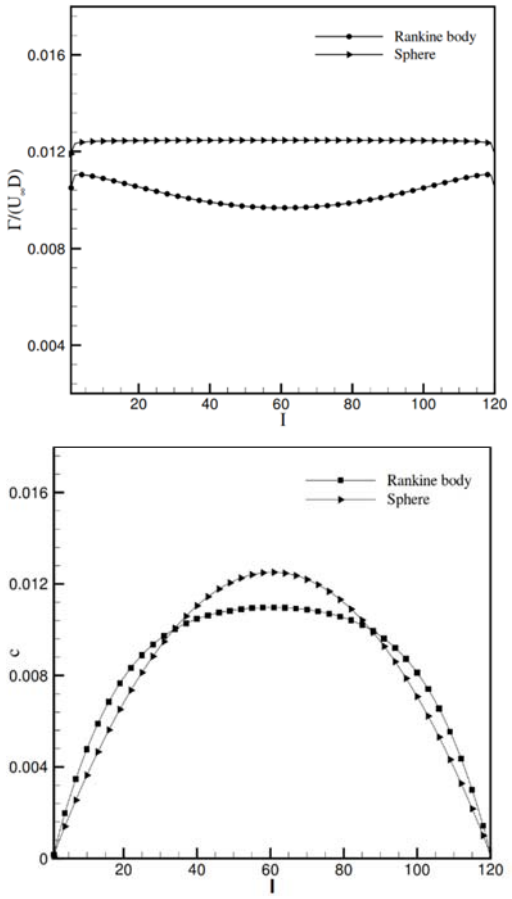

Fig. 6. (a) Circulation and (b) contribution of each vorticity loop of the Rankine body and the sphere.

Then the Rankine body is compared with a droplet type body displayed in Fig. 7 for investigating the influence of the trailing edge type, where the fineness ratio of the droplet type body is set to 2. The only different between the two bodies is that the Rankine body is rounded on the trailing edge while the droplet type body is sharply tapered at the trailing edge. The droplet type body is approximated by 120 vorticity loops and the apparent mass coefficient of the body in the axial direction is 0.2264 calculated by the new method, which is larger than that of the Rankine body. Additional, it is important to remind that, for the droplet body whose closed form of velocity potential function does not exists, the apparent mass can not be derived directly using potential flow method.

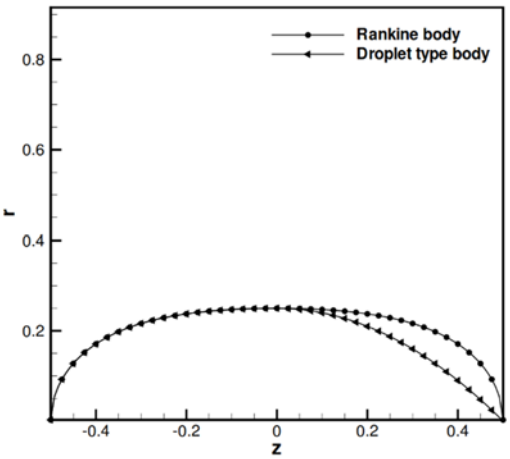

Fig. 7. Profiles of the Rankine body and the droplet type body.

Fig. 8(a) shows the circulation of each vorticity loop of the Rankine body and the droplet type body. The circulation of vorticity loops located at the foreparts of the both bodies are almost same which means the vorticity distribution of the vorticity loops located at the forepart won't be affected by the change of the trailing edge type. Compared with the Rankine body, although the sharped trailing edge decreases the circulation of the vorticity loops located at the latter part, it increases the circulation of the loops located at the middle part. The area of the vorticity loop located at the middle part is much larger than the loop located at the latter part, so the total apparent mass of the droplet body is larger than that of the Rankine body. Fig. 8(b) shows the contribution of each loop of the both bodies. The contribution of the vorticity loops located at the forepart of the droplet type body are larger than that of the Rankine body, whereas the contribution of the vorticity loops located at the latter part of the droplet type body are smaller than that of the Rankine body.

The above discussion based on the new method has revealed some physical mechanism of the apparent mass which can not be obtained by the potential flow method.

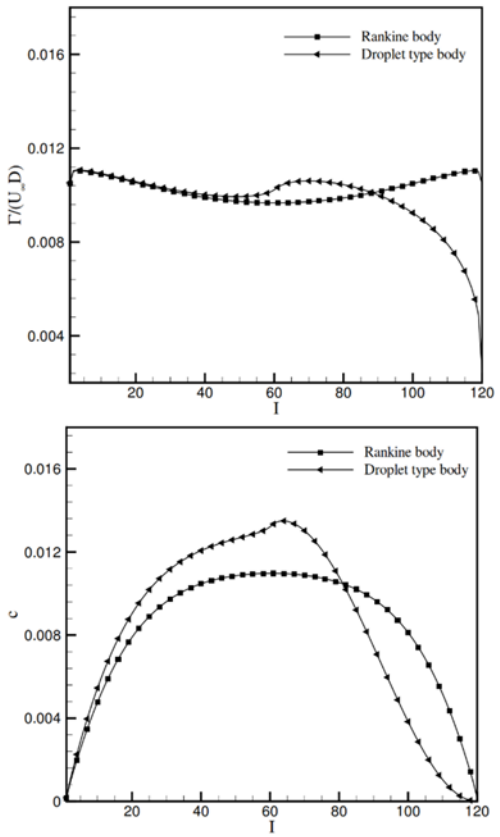

Fig. 8. (a) Circulation and (b) contribution of each vorticity loop of the Rankine body and the droplet type body.

6. CONCLUSION

In this paper, a new method based on vorticity moment theorem for calculating the apparent mass of the revolution body in the axial direction due to axial acceleration is presented. Compared with the traditional methods, the new method does not adopt the concept of the ideal flow which is not realistic in real flow field. Using the new method, the apparent mass of an arbitrary body of revolution in the axial direction can be easily figured out and the physical mechanism of the apparent mass can be revealed from the view of the vorticity loops adjacent to the surface of the body. The apparent mass coefficients of a sphere and a Rankine body were calculated out by the new method and shown a good agreement with the results obtained by the potential flow method.

With the help of the new method, two features of the apparent mass have been explained. First, a smaller fineness ratio corresponding to larger areas of vorticity loops induces a larger circulation distribution, so a larger apparent mass coefficient can be obtained. Second, the vorticity distribution of the vorticity loops located at the forepart won't be affected by the change of the trailing edge type, the change of the total apparent mass comes from the change of the circulation and area of loops located at the trailing edge itself. These characteristics are very useful when it is need to change the apparent mass of airship or aircraft.

ACKNOWLEDGMENTS

The financial support of the National Key Technology Support Program (2015BAA06B04-2) is greatly acknowledged.

REFERENCES

Birkhoff (1960). *Hydrodynamics*. Princeton, USA.: Princeton University Press.

Korotkin, A. I. (2007). *Added masses of ship structures*. St. Petersburg, RUS.: Springer.

Lamb (1932). *Hydrodynamics*. Cambridge, UK.: Cambridge University Press.

Li, G. J. and X. Y. Lu (2012). Force and power of flapping plates in a fluid. *Journal of Fluid Mechanics 712*, 598–613.

Li, J. and Z. N. Wu (2016). A vortex force study for a flat plate at high angle of attack. *Journal of Fluid Mechanics 801*, 222–249.

Li, Y. and M. Nahon (2007). Modeling and simulation of airship dynamics. *J. Guidance, Control, and Dynamics 30*(6), 1691–1700.

Lighthill (1986). *An Informal Introduction to Theoretical Fluid Mechanics*. Oxford, UK.: Oxford University Press.

Milne-Thomson, L. M. (1968). Theoretical hydrodynamics. NewYork, USA.: Macmillan. Rayner, J. M. V. (1979). A vortex theory of animal flight. part 1.the vortex wake of a hovering animal. *Journal of Fluid Mechanics 91*(04), 697–730.

Sane, S. P. and M. H. Dickinson (2002). The aerodynamic effects of wing rotation and a revised quasi-steady model of flap-ping flight. *Journal of experimental biology 205*(8), 1087–1096.

Smith, A. M. O. and J. Pierce (1958*). Exact so- lution of the neumann problem. calculation of plane and axially symmetric flows about or within arbitrary boundaries*. Douglas Air-craft Company Report (26988), 807–815.

Tian, W., A. Bodling, H. Liu, J. C. Wu, G. He and H. Hu (2016). An experimental study of the effects of pitch-pivot-point location on the propulsion performance of a pitching airfoil. *Journal of Fluids and Structures 60*, 130–142.

Wang, X. X. and Z. N. Wu (2010). Stroke- averaged lift forces due to vortex rings and their mutual interactions for a flapping flight model. *Journal of Fluid Mechanics 654*, 453–472.

Wu, J. C. (1981). Theory for aerodynamic force and moment in viscous flows. *AIAA Journal 19*(4), 432–441.

Wu, J. C. (1986). *Elements of vorticity aerodynamics*. Beijing, China, Tsinghua University Press.